Ultrasound-based navigated pedicle screw insertion without intraoperative radiation: feasibility study on porcine cadavers

Background: Navigation systems for spinal fusion surgery rely on intraoperative computed tomography (CT) or fluoroscopy imaging. Both expose patient, surgeons and operating room staff to significant amounts of radiation. Alternative methods involving intraoperative ultrasound (iUS) imaging have recently showed promise for image-to-patient registration. Yet, feasibility and safety of iUS navigation in spinal fusion have not been demonstrated.

Purpose: To evaluate the accuracy of pedicle screw insertion in lumbar and thoracolumbar spinal fusion using a fully automated iUS navigation system.

Study Design: Prospective porcine cadaver study.

Methods: Five porcine cadavers were used to instrument the lumbar and thoracolumbar spine using posterior open surgery. During the procedure, iUS images were acquired and used to establish automatic registration between the anatomy and preoperative CT images. Navigation was performed with the preoperative CT using tracked instruments. Accuracy of the system was measured as the distance of manually collected points to the preoperative CT vertebral surface and compared against fiducial-based registration. A postoperative CT was acquired, and screw placements were manually verified. We report breach rate, as well as axial and sagittal screw deviations.

Results: A total of 56 screws were inserted (5.50 mm diameter $\mathrm{n} = 50$, and 6.50 mm diameter $\mathrm{n} = 6$). Fifty-two screws were inserted safely without breach. Four screws (7.14%) presented a medial breach with an average deviation of $1.35 \pm 0.37\ \mathrm{mm}$ (all $< 2\ \mathrm{mm}$). Two breaches were caused by 6.50 mm diameter screws, and two by 5.50 mm screws. For vertebrae instrumented with 5.50 mm screws, the average axial diameter of the pedicle was 9.29 mm leaving a 1.89 mm margin in the left and right pedicle. For vertebrae instrumented with 6.50 mm screws, the average axial diameter of the pedicle was 8.99 mm leaving a 1.24 mm error margin

in the left and right pedicle. The average distance to the vertebral surface was 0.96 mm using iUS registration and 0.97 mm using fiducial-based registration.

Conclusions: We successfully implanted all pedicle screws in the thoracolumbar spine using the ultrasound-based navigation system. All breaches recorded were minor (<2 mm) and the breach rate (7.14%) was comparable to existing literature. More investigation is needed to evaluate consistency, reproducibility, and performance in surgical context.

Clinical significance: Intraoperative US-based navigation is feasible and practical for pedicle screw insertion in a porcine model. It might be used as a low-cost and radiation-free alternative to intraoperative CT and fluoroscopy in the future.

Keywords: Ultrasound, Image-guided surgery, Fusion surgery, Screw insertion, Radiation-free navigation

1 Introduction

Insertion of pedicle screws in lumbar spine, either free-hand or under fluoroscopy guidance, is associated with a small but significant risk of breaches that can have both neurological and vascular repercussions on patient outcomes [1], [2], [3]. Image-guided surgery (IGS) uses tracked instruments to provide live visualization of the screw trajectory. Pre-surgical plan, with optimal entry points and angular orientations, can thus be brought to the patient to reduce breach risks [4]. The navigation process requires that the preoperative images and surgical plan to be aligned to the patient anatomy during surgery. Existing systems, such as the O-arm (Medtronic inc., Minneapolis, MN, USA), are based either on intraoperative 2D fluoroscopy navigation, or intraoperative 3D computed tomography (CT) imaging for IGS navigation. While intraoperative CT-based IGS provides automatic registration and updates anatomical images, the procedure introduces significant costs and requires necessary but counter-productive surgical workflow interruptions, typically lasting 10–20 minutes for setup and scanning. Although intraoperative CT navigation reduces exposure to ionizing radiation compared to fluoroscopy, the amount of radiation exposure to patient and staff is still significant [48].

Alternative approaches have considered intraoperative ultrasound (iUS) imaging. Early work in spine surgery has focused on using iUS without instrument tracking, for example in spinal canal decompression [5] and fracture fragments repositioning [6]. Ultrasound images were only used to visually assess local anatomy, e.g., bone fracture, or spinal cord. Recently, iUS-based IGS, in which the procedure consists of using tracked ultrasound images to establish registration and to navigate on preoperative images, has received growing interest for spinal interventions as registration algorithms are becoming more robust, accurate and efficient [7]. Nevertheless, iUS-based IGS has not been established as the norm in the operating room (OR) for spine surgery. Among factors hindering deployment of this technology in the OR is the lack of clinical validation. So far, most of the work emphasizes on evaluating the registration quality using plastic phantoms [8], [9], [10], ex vivo spine anatomy [11], or animal cadavers including sheep [12], [13], [14] and pigs [15], [16], [17], [18], [19]. The few papers evaluating feasibility on clinical data have focused on needle guidance applications [20], [22], [22], [23]. Although Winter et al. [24] evaluated their

method on data collected on 5 patients undergoing surgery, their validation was limited to assessing the registration robustness. There is a need to understand the role and the contribution of iUS-based IGS in spine surgery, especially regarding its integration in the surgical workflow as well as its usability during surgery.

In our previous work, we developed a software for pedicle screw navigation that uses iUS-based IGS and investigated the accuracy, robustness, and computation time of the system [25]. Our system achieves image registration with an accuracy of 1.47 mm in 10 seconds, and when combined with the necessary iUS acquisition, enables navigation in one to two minutes of intraoperative time. Once the registration completed, navigation is performed on preoperative CT images, robustly aligned to the patient's anatomy. In this study, we evaluated the use of our system for the insertion of pedicle screws in a porcine thoracolumbar spine.

2 Materials and Methods

2.1 Navigation system

The IGS system comprises three elements: a tracking camera, an ultrasound scanner and a computer workstation (Fig. 1). The navigation operates on the IBIS software v.3.6.0 (http://ibisneuronav.org) [26], an open-source neuronavigation platform that provides common navigation functionalities such as 3D data visualization, ultrasound probe calibration using a 3D printed phantom, ultrasound acquisitions and volume reconstruction. The PLUS toolkit [27] was used to stream data between IBIS and the hardware devices, i.e., ultrasound and tracking camera. Intraoperative ultrasound was acquired using a BK3500 system (BK Medical, Peabody, MA, USA), equipped with a N13C5 curved probe. The N13C5 probe has a contact surface of 29 mm $\times$ 10 mm, small enough to fit inside the surgical cavity. Although linear probes have a higher frequency and better depth image quality, early experimentation with a linear probe showed some limitations regarding the field of view, especially for imaging lateral parts of the vertebra. During navigation, the probe and surgical instruments are tracked using a *FusionTrack 500* camera (Atracsys, Puidoux, Switzerland). This tracking camera determines the spatial location of infrared light-reflecting spheres rigidly fixed to the tracked tools. In this study, the tracked instruments consist of a planar blunt probe PN960-556 (Medtronic, Dublin, Ireland) used as a navigation

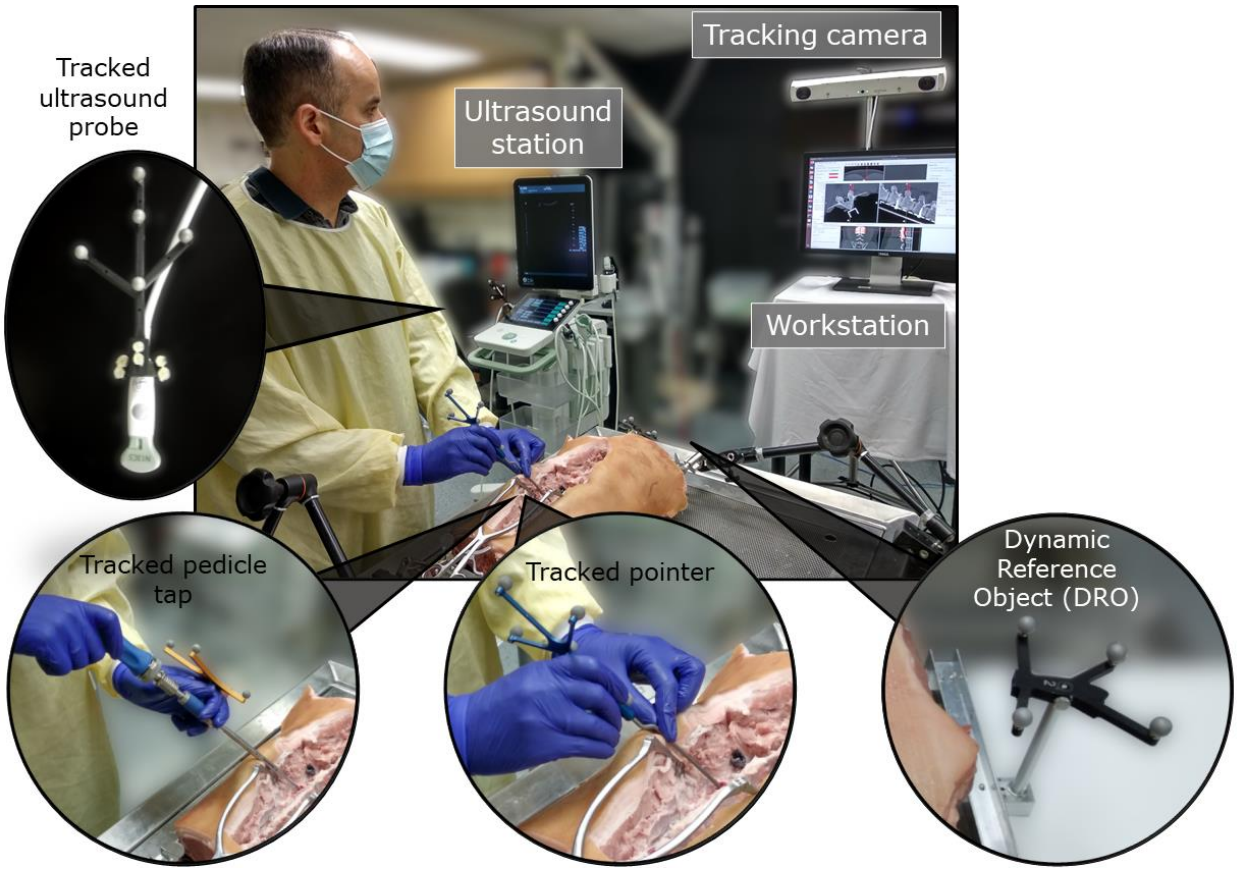

Figure 1. Ultrasound-based image-guided surgery system: the N13C5 ultrasound probe, the pedicle tap and the planar blunt probe (pointer) are tracked with respect to the dynamic reference object.

pointer, a non-cannulated 4.50 mm navigated tap (Medtronic) used to create the screw channel, and the iUS probe used for registration. Note that additional navigated instruments can be further included to the navigation system, but this was not considered in this study.

The iUS-based navigation protocol requires three major steps. First, a preoperative CT scan must be obtained and the images are automatically segmented to extract the posterior surface of the vertebrae needed for registration. Second, the posterior elements of the spine should be exposed surgically and a dynamic reference object (DRO), used as the navigation reference, is attached to an element with a fixed spatial relationship compared to the instrumented vertebrae (e.g., usually the spinous process of the instrumented or adjacent vertebra, but not in our experiment as explained below). This step is common among all navigation systems (e.g., CT-based IGS) and is used to prevent errors caused by patient displacement during the intervention. Finally, the cavity must be filled with a saline solution and an iUS scan obtained. The iUS images are used to establish registration between patient anatomy and preoperative CT images, and

thus enable navigation on the latter images. Note that ultrasound images are not used to navigate, but only to collect anatomical features for registration.

2.2 Porcine cadaver preparation, instrumentation and preoperative imaging

The navigation system was evaluated on the thoraco-lumbar section of porcine cadavers in which at least the last thoracic, all lumbar vertebrae (T15 and L1-L6 for porcine spines) and sacrum were present. The cadaver consisted of a complete pork loin, with spine, purchased from a local butcher. On the first day, the cadaveric porcine spine was fixed in prone position to an aluminum frame to prevent intervertebral motion. The iUS probe calibration was performed prior to surgery using IBIS [28]. A rigid body containing 4 infra-red reflective spheres was attached to the frame and serves as DRO. A preoperative CT scan was performed with a clinical scanner (Aquilion ONE, Canon Medical, Japan) at a slice resolution of 0.5×0.5 mm^2 and a slice thickness of 0.5 mm. Note that the reflective spheres of the DRO are clearly visible on CT images and can be used as fiducials to establish the gold-standard registration. The CT images were manually divided into sub-volumes corresponding to each vertebra using 3D Slicer software v.4.11.0 (www.slicer.org) [29]. Note that this experimental protocol involves additional steps that are not required for iUS-based IGS. However, they aim to provide a controlled environment for the assessment of the system. More specifically, the DRO is attached prior to CT acquistion, and thus used to provide gold-standard alignment used to obtain a reference registration for comparison. Fixing the spine to the aluminium frame prevents intervertebral motion and reduces sources of error and bias caused by changes in the spine curvature.

On the second day, the posterior elements of the vertebrae were exposed from the thoracolumbar junction to the sacrum. The surgical cavity was filled with water and an iUS scan was performed. The iUS acquisition was performed as a single sweep in the caudo-cranial direction, starting from the inferior to the superior parts of each vertebra separately. The images are automatically streamed to IBIS to perform the registration with the preoperative CT. In practice, the registration accuracy is satisfactory (below 2 mm) for adjacent vertebral levels and decreases linearly as we move farther from the registered level [19]. However, for the experiments reported here, the iUS acquisition and registration procedures were repeated once

for each vertebra.

Before instrumentation, the alignment between the iUS and the preoperative CT images was visually inspected on the screen during the registration step. Moreover, qualitative assessment of the navigation was performed by pin-pointing the tip of the spinous process and the articular joints with the navigated pointer to ensure that the corresponding anatomical landmarks are targeted on the CT images. In the case where the registration was not satisfactory, a new iUS acquisition was performed and the registration was computed again. The acquisition lasts between 30-60 seconds and the computations require less than 10 seconds to obtain a new registration enabling quick re-registration when needed without significantly interrupting the surgical workflow.

Once the registration completed, navigation was possible on preoperative CT images using the pointer or the pedicle tap. The navigated pointer was used to determine the entry point and trajectory for the insertion of the pedicle screw and a navigated pedicle tap was used to prepare the trajectory of the screw, which was then inserted with a non-navigated screwdriver. Figure 2 shows a snapshot of axial and sagittal navigation views during screw insertion. The entry point was created with a Leksell rongeur and the initial few millimetres of the trajectory with a pedicle awl and a pedicle finder based on a trajectory previously shown using the navigated pointer. Screws of two diameters were used depending on the size of the pedicle: 5.50 mm and 6.50 mm.

Figure 2. IBIS software: Snapshot from intraoperative use of navigated tap. The tool tip and the expected screw trajectory are shown in solid red lines, and the saved trajectory is shown in dotted lines.

2.3 Registration accuracy

We compared the automatic registration transformation obtained using iUS against a reference registration transformation obtained by identifying the center of the reflective spheres attached to the DRO on the preoperative CT images. For the reference transform, each sphere was manually segmented, and the corresponding center of mass was used as the fiducial position. Because both the porcine cadaver and the DRO are rigidly fixed to the aluminum frame, the spatial relationship between the DRO and the anatomy is assumed to be invariant. Therefore, establishing the pairwise correspondence between the position of the DRO spheres (known by construction) and the position of the fiducials on the CT images allows us to compute the alignment between the tracked tools and the images, which is used as the gold-standard reference transform. This procedure is similar to the one used by commercial intraoperative CT-based IGS systems, with the difference that the fiducials are placed closer to the instrumented vertebra and that they are automatically identified on CT images.

Registration accuracy was measured as the *point-to-surface registration error*. This metric represents the distance between points collected on the anatomical surface of the vertebra and the surface extracted from CT images. For each instrumented vertebra, 4 to 9 points located on the posterior surface were collected with the navigated pointer. These points represent the *anatomical surface* and were roughly equally distributed on the exposed vertebra: 1-2 points on the tip of the spinous process, 2-4 points on the left and right laminae, and 2-4 points on the left and right articular joints. Then, we manually segment the posterior vertebral surface on CT images using the method described by Yan et al. [30]. The resulting segmentation is converted to a mesh [31] and projected into the registered space using either the iUS registration or the gold-standard reference transform. Finally, for each anatomical surface point, we compute the distance to the closest point lying on the projected mesh, referred to as registration error.

2.4 Breach assessment

After the insertion of the pedicle screws a postoperative CT scan was performed to evaluate the actual position of the implanted screws on a DICOM viewer (RadiAnt viewer, Medixant, Poznan, Poland). Image resolution and slice thickness were the same as for the preoperative scan,

i.e., 0.5×0.5 mm² and 0.5 mm, respectively. The maximum deviation of the breach in whichever plane present was measured in millimetres from the closest parallel point of the pedicle as described in the literature [32]. A screw is considered breaching if it violates the cortex of pedicle or vertebral body at any direction (apart from the entry point). We use the 2-mm increment for breach classification [33], [34]: 1) *no breach*, if the screw is inside pedicle, 2) *mild breach*, if the screw deviation is < 2 mm, and 3) *major breach*, if the screw deviation is ≥ 2 mm.

2.5 Pedicle measurement

Using the preoperative CT and the DICOM viewer, we measured the axial and sagittal pedicle sizes of each instrumented vertebra. For the axial measurements we used the original DICOM axial plane; whereas for the sagittal measurements, the sagittal plane was slightly reformatted to match the pedicle orientation. For each plane, we measured the diameter of the pedicle from cortex to cortex on multiple slices located in the middle of the pedicle. The slice with the largest pedicle diameter was used to obtain the final measurement.

3 Results

The system was successfully used to establish navigation for 28 vertebrae in five porcine cadavers. A total of 56 screws were inserted: 50 screws had a diameter of 5.50 mm and 6 screws had a diameter of 6.50 mm. Out of the 56 screws, 52 screws (92.86 %) were inside the pedicle, only 4 screws (7.14 %) presented mild breaches, and no major breaches were observed. The reported breaches were all medial and were located at left T15 (cadaver #1, 1.36 mm), left L5 (cadaver #3, 0.70 mm), right L2 (cadaver #3, 0.80 mm), and right L1 (cadaver #5, 1.37 mm). No lateral, anterior, inferior or superior breaches were observed. Among the 4 breaches, 2 were caused by a 6.50 mm diameter screw and 2 by a 5.50 mm diameter screw. Table 1 summarizes breach results per vertebral level and Fig. 3 shows postoperative CT scans of breaching screws

Table 1. Summary of screw insertion results

		Breaches		
Vertebral level	Number of screws	Number of breaches	Type	Deviation (mm)
L6	2×6.50 mm	0		
L5	4×5.50 mm, 2×6.50 mm	1	Medial	0.70
L4	10×5.50 mm	0		
L3	10×5.50 mm	0		
L2	10×5.50 mm	1	Medial	0.80
L1	10×5.50 mm	1	Medial	1.37
T15	4×5.50 mm, 2×6.50 mm	1	Medial	1.36
T14	2×5.50 mm			
Total	56	4 (7.14 %)	4×medial	1.06±0.31 mm

The 5.50 mm and 6.50 mm indicate screw diameters.

and examples of non-breaching screws.

We measured pedicle diameters of the instrumented vertebrae in axial and sagittal views and the results are shown in Table 2. The size of the pedicles was similar across the specimens with little variation. The average pedicle diameter was 9.26 ± 0.61 mm in the axial view and 15.65 ± 0.89 in the sagittal view. For vertebrae instrumented with a 5.50 mm screw, the average axial diameter was 9.29 mm leaving 1.89 mm margin in left and right pedicles, and the average sagittal diameter was 15.71 mm leaving 5.10 mm margin in superior and inferior pedicles. For vertebrae instrumented with a 6.50 mm screw, the average axial diameter was 8.99 mm leaving 1.24 mm error margin in left and right pedicles, and the average sagittal diameter

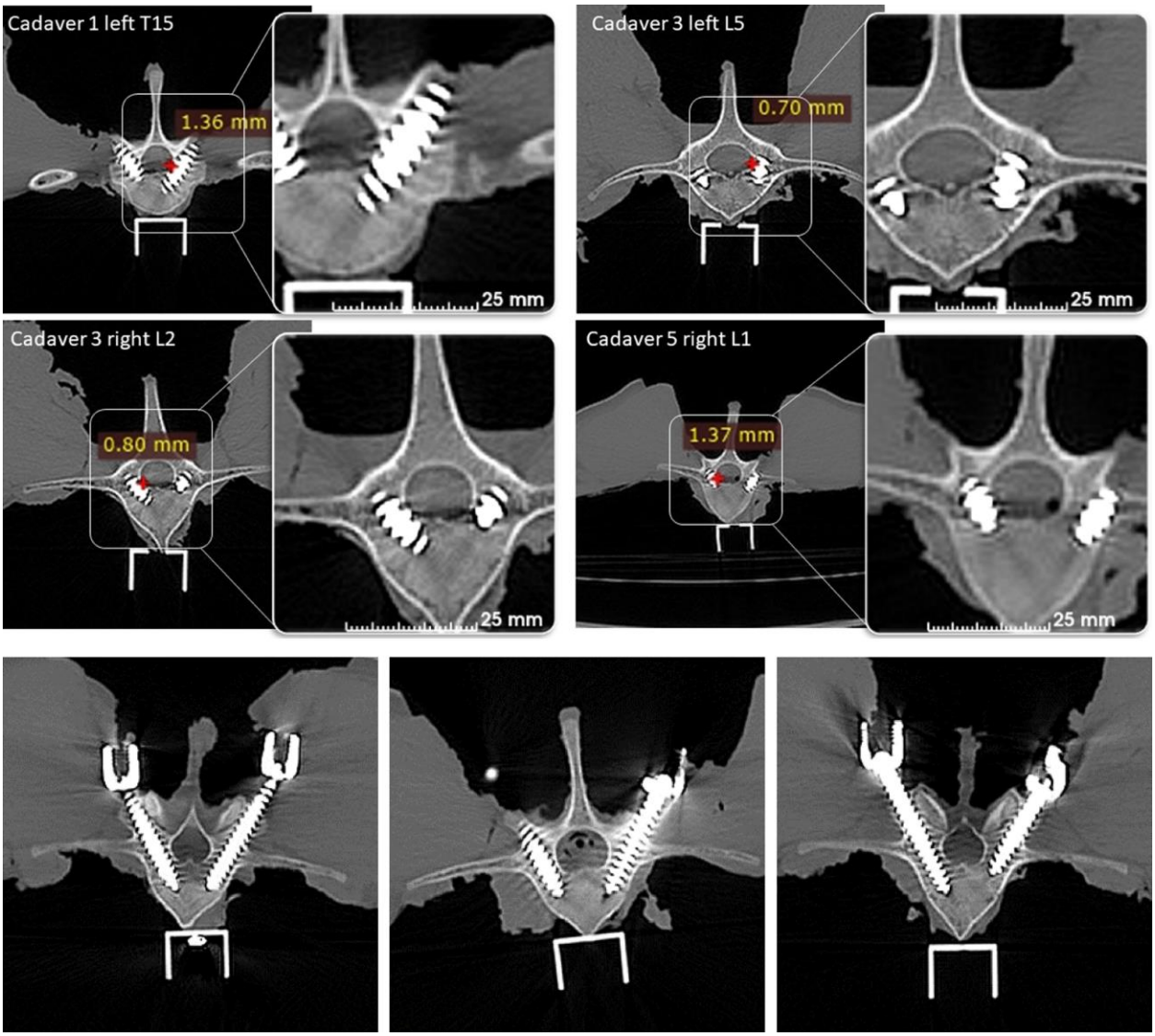

Figure 3. Postoperative CT scans: (a) axial view of breaching screws, and (b) examples of screws inside the pedicle, axial view reformatted along the screws.

was 15.11 mm leaving 4.30 mm error margin in superior and inferior pedicles.

Among the 28 instrumented vertebrae, the registration failed to align CT to iUS images on the first attempt in 6 vertebrae (21.4 %): cadaver #1 at L2, cadaver #2 at L5, cadaver #3 at L3, cadaver #4 at L1 and L4, and cadaver #5 at L3. In these cases, a new iUS scan was acquired and the registration was successfully performed yielding 100% success for all 28 vertebrae.

Table 2. Pedicle diameter of the porcine cadavers in axial and sagittal views

	Axial (mm)	Sagittal (mm)
Level	Mean±Stand. dev.	Mean±Stand. dev.
L6	8.19±0.52	16.25 ± 0.64
L5	9.64±0.53	14.92 ± 1.58
L4	9.09±0.59	15.44 ± 0.88
L3	9.08±0.61	15.90 ± 0.79
L2	9.48±0.52	15.76± 0.83
L1	9.51±0.45	16.04± 0.46
T15	8.80±0.56	15.68±0.33
T14	9.87±0.15	14.45±0.49
All	9.26±0.61	15.65±0.89

Table 3 summarizes registration errors for both iUS registration and the gold-standard reference registration. Box plots of registration errors per individual vertebral level are shown in Fig. 4. The average registration error was 0.96 mm using the iUS registration and 0.97 mm using the gold-standard reference registration.

4 Discussion

4.1 Breach evaluation

The proper placement of screw insertion is typically verified on X-ray or CT images, if possible before closing the wound, to allow misplaced screws to be corrected. However, in general, not all breaches would be considered for repositioning by all spine surgeons [35]. Such a decision depends on several factors involving the appearance of new postoperative symptoms, the sensitivity of the imaging modality, the deviation and location of the breach, and the vertebral level, with lumbar spine having more room for displacement of thecal sac and nerve roots. There is no established standard for breach assessment, but most methods use the 2 mm-increment

Table 3. Results of registration error for both iUS registration and gold-standard registration

	Registration error (mm)			
	iUS		Gold-standard	
Cadaver	Mean	Median ± IQR	Mean	Median±IQR
1	1.14	0.85 ± 0.82	0.82	0.59±0.60
2	0.67	0.62 ± 0.47	0.83	0.68±0.67
3	0.88	0.65 ± 1.00	0.89	0.60±1.21
4	0.86	0.83 ± 0.77	1.12	0.88±1.02
5	1.03	0.84±0.72	1.16	0.75±1.12
Average	0.96	0.73± 0.79	0.97	0.71± 0.98

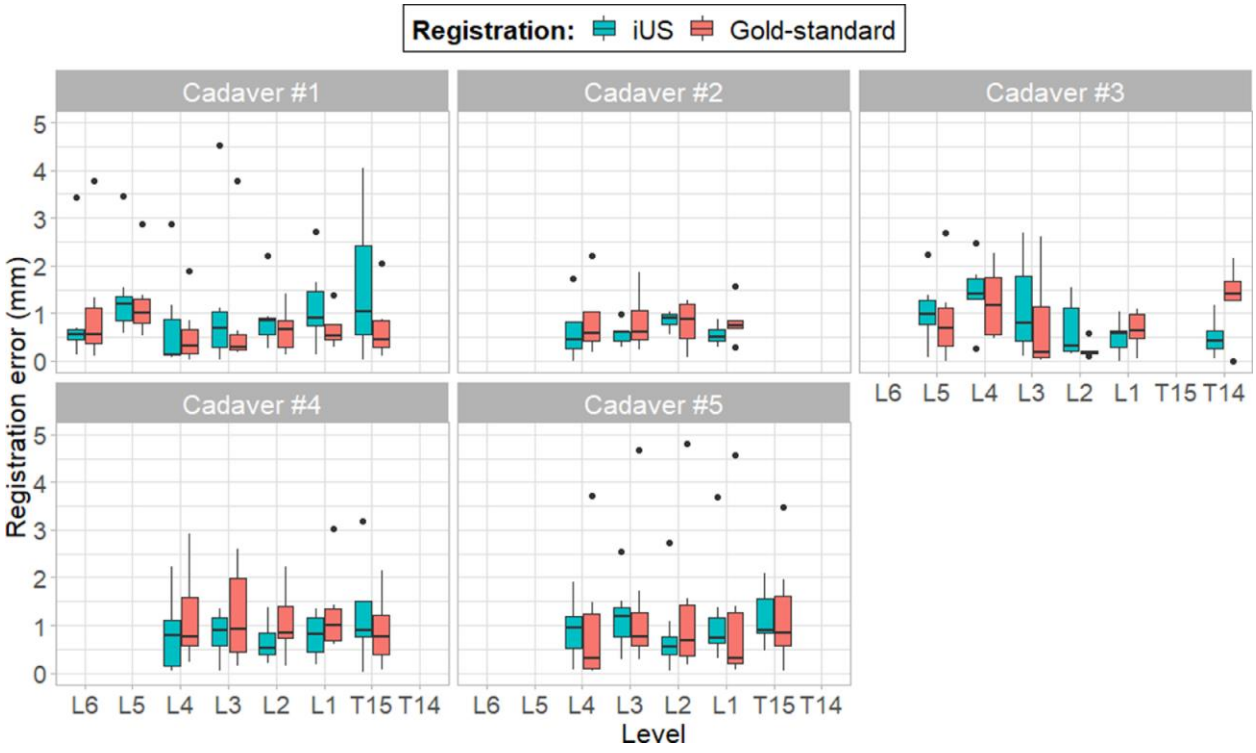

Figure 4. Results of accuracy measured as registration error for iUS vs. gold-standard registration.

technique to classify breaches into [32]: < 2 mm which usually is clinically safe for lumbar spine, 2-4 mm, 4-6 mm and > 6 mm. All breaches in our study were medial, but minor (<2 mm).

Furthermore, the breach rate of 7.14%, which was similar to the rate reported in the literature for CT navigated spinal fusion 2 %–11.4 % [36], [37], [38], [39], [40].

4.2 System accuracy

In lumbar spine, the technical accuracy requirement for image-guided spinal fusion is 1-2 mm [41], [42]. In our study, both the iUS registration and the gold-standard transform yielded a sub-millimetric average accuracy, with no significant difference between methods. In this experiment, a few important observations are noted. First, the reference alignment was obtained using DRO fiducials placed at the "caudal" edge of the aluminum frame next to the sacrum, causing any error in the fiducial localization to amplify registration error as the distance from the DRO increases [43]. The instrumented vertebrae were located from 20 to 40 cm away from the DRO. Note that this is specific to the setup used in our experiment and is unlikely to be the case in surgery where the DRO is usually placed on the vertebra adjacent to the instrumented level, e.g., when using intraoperative CT-based IGS. Nevertheless, the accuracy results (mean registration error of 0.97 mm) obtained with the gold-standard transform are below the required 2 mm, indicating that the alignment is sufficiently good for navigation.

Second, because of the ligaments and soft tissue present on the vertebra surface, some of the anatomical surface points collected with the navigated pointer had a slight offset with respect to the true bone surface, even more so for points located on the spinous process. It is also important to note that there might be a slight bias in the segmentation of the vertebral surface, inwards or outwards from the true surface. However, if it exists, this bias would affect the evaluation of the gold-standard registration and the proposed iUS registration in a similar way. In addition, potential bias was reduced because the same set of tracked points was used to compute the accuracy of iUS registration and gold-standard registration, enabling a direct comparison of the accuracy results.

Third, both registration methods are equally affected by the accuracy in identifying the DRO spheres and by the tool tracking accuracy of the planar blunt probe and the navigated tap. Both of these factors add equally to the registration error of both methods.

Finally, the proposed system is dependent on iUS calibration. Any errors in calibration will

be propagated into the proposed iUS registration transformation. Accuracy of the iUS calibration was shown to vary between 0.49 and 0.82 mm [28] and in our experiments, the average registration error obtained with iUS registration is similar to the one obtained with the gold-standard transform. We conclude that the accuracy of both approaches is comparable in these experiments.

4.3 Porcine anatomy

Lumbar spines of porcine cadavers are commonly used in validation and training for spinal instrumentation [44], [45]. Although similar to human spine, a few differences exist. The porcine specimens have typically 6 lumbar and 15 thoracic vertebrae. The most caudal vertebra L6 is smaller than other vertebrae, its pedicles have a very medial orientation, is difficult to access for instrumentation, and overall not very similar to the human lumbar vertebrae. Thus, it has been mostly discarded in our study. Most importantly, the pedicles of the porcine lumbar spine have a more cranio-caudal angulation than in the human anatomy. In general, these differences contributed to reduce the bias related to the surgeon's experience, driving the results to be more focused on the IGS system.

Regarding pedicle size, there was very little variation of the measurements in the thoraco-lumbar spine of the instrumented vertebrae, i.e., T14-L5. The average pedicle size was 9.26 $\pm$ 0.61 mm in axial view and 15.65 $\pm$ 0.89 mm in sagittal view. In human spine, pedicle width in the axial view can be slightly smaller: 6-7 mm in T12, L5 and L4, and similar or larger for L1-L3: 9-17 mm. In sagittal plane, it is typically similar or smaller: 12-15 mm [46]. These differences are usually managed by adapting the screw diameter and length to the patient's anatomy.

4.4 Potential Clinical Advantages

The proposed technique requires registration to a pre-operative CT for navigation. In many cases, such a scan is already available for other medical reasons, e.g., imaging for diagnosis, evaluation of hardware and fusion regarding previous interventions, or evaluation of adjacent segment disease for instrumentation extension. Like the manual landmark-based registration systems, the proposed iUS registration method obviates the need for intraoperative fluoroscopy

or O-arm imaging used in many navigation systems. Taking only a minute or two, the proposed iUS registration is faster than both manual registration techniques and other radiation-based imaging solutions. Finally, ultrasound is commonly used for other intraoperative neurosurgical applications, such as evaluation of the location and removal of tumors and assessment of the decompression of the anterior surface of the spinal cord. The proposed method can thus take advantage of existing equipment with the significant investment required for other navigation solutions based on fluoroscopy or O-arm imaging. Further evaluation in human patients will be necessary to evaluate its true potential.

4.5 Limitations

The use of iUS navigation for spine surgery is still under investigation, especially regarding clinical validation. The present study was purely experimental and did not involve surgical conditions, such as exposure to surgical field, stability of structures, blood, soft tissue and neural structures. Such conditions would help identifying limitations of the new iUS-based IGS in the clinical context, but are difficult to reproduce experimentally, especially at this early stage. In addition, spinal deformity, and presence of hardware due to previous fusions may have an impact on the performance of the navigation system. This study was limited to non-pathological spine. Furthermore, the proposed iUS system does not allow evaluation of pedicle placement, in contrast to standard intraoperative imaging, e.g., fluoroscopy or O-arm. There have been studies demonstrating feasibility of intrapedicular breach evaluation using micro-ultrasound probe designed to fit inside the pedicle hole [49][50][51], but this is beyond the scope of this study. Moreover, while there are benefits of using iUS in the context of minimally invasive spine surgery, the system was only evaluated on open exposures, limiting the results to feasibility in open spine surgery. Further research involving real patient data is needed to explore the integration of the system to the current surgical workflow and its usability for percutaneous screw insertion.

The registration failed to properly align CT to iUS images in the case of low iUS image quality. We have not been successful in identifying the exact conditions that yielded poor acquisitions. We believe that this could be due to a lack of anatomical features in the acquired images, an iUS sweep acquired too quickly, or an iUS probe trajectory that violates the acquisition protocol. The

latter plays a role in initializing the registration and a failure in this step could prohibit algorithm convergence. Nevertheless, these cases were easily identified by visually inspecting the aligned images, as the resulting misalignment was obvious. In clinical context, this could be corrected by re-acquiring iUS images without difficulty. Computation time is sufficiently fast (under 10 seconds) to allow alignment inspection before removing the saline solution from the cavity, thus enabling a quick iUS rescan.

By fixing the cadaver to a rigid frame, we assume that no intervertebral motion occurred between preoperative and intraoperative imaging. While this enables the establishment of a gold-standard reference transform using the DRO, it limits the validation to the context of rigid registration. In a clinical context, the patient is often in supine position for preoperative CT and in prone position during the surgery. Hence, the spine curvature is subject to variations that may not be corrected with a single rigid registration for all vertebrae. Registering one vertebral level at a time, as performed in our experiment, eliminates spine curvature errors. Note that this is only practical when the registration procedure is sufficiently fast to not overburden the surgical workflow. While it is possible to account for spine curvature by performing a group-wise rigid registration of multiple vertebral levels [12], [13], [47], these methods require 15-40 min to complete the registration, which is not applicable in the OR.

Finally, in our experiment, the slice thickness of preoperative CT was 0.5 mm. While this yields a fine image resolution of the final reconstructed CT volume that is used for registration and navigation, the typical slice thickness in clinical context is 2-3 mm. The latter parameters result in coarse image resolution, usually in the sagittal view, that may affect registration accuracy and navigation efficacy. Further investigations need to be conducted regarding the role of imaging parameters in the navigation system.

5 Conclusion

In this study, we successfully implanted 56 screws in the thoracolumbar spine using the navigation system. No intraoperative ionizing radiation imaging was involved during surgery. Out of the 56 screws, only 4 screws resulted in breaches, a breach rate similar to that reported in the literature using commercial IGS systems. All breaches measured less than 2 mm and most

probably would neither have caused symptoms, nor have required revision surgery. Future research should focus on usability and safety of the system under real surgical conditions. We believe iUS-based IGS may help reduce surgery time and radiation exposure in the OR.

References

[1] M. S. Austin, A. R. Vaccaro, B. Brislin, R. Nachwalter, A. S. Hilibrand, T. J. Albert, Image-Guided Spine Surgery A Cadaver Study Comparing Conventional Open Laminoforaminotomy and Two Image-Guided Techniques for Pedicle Screw Placement in Posterolateral Fusion and Nonfusion Models, Spine 27 (2002) 2503–2508.

[2] Y. Aoki, M. Yamagata, F. Nakajima, Y. Ikeda, K. Shimizu, M. Yoshihara, J. Iwasaki, T. Toyone, K. Nakagawa, A. Nakajima, et al., Examining risk factors for posterior migration of fusion cages following transforaminal lumbar interbody fusion: a possible limitation of unilateral pedicle screw fixation, Journal of Neurosurgery: Spine 13 (2010) 381–387.

[3] Z. A. Smith, K. Sugimoto, C. D. Lawton, R. G. Fessler, Incidence of Lumbar Spine Pedicle Breach After Percutaneous Screw Fixation A Radiographic Evaluation of 601 Screws in 151 Patients, Journal of Spinal Disorders and Techniques 27 (2014) 358–363.

[4] F. Gebhard, A. Weidner, U. C. Liener, U. Stöckle, M. Arand, Navigation at the spine, Injury 35 (2004) 35 – 45.

[5] K. Lerch, M. Völk, G. Heers, W. Baer, M. Nerlich, Ultrasound-guided decompression of the spinal canal in traumatic stenosis, Ultrasound in medicine & biology 28 (2002) 27–32.

[6] L. A. Mueller, J. Degreif, R. Schmidt, D. Pfander, R. Forst, P. M. Rommens, L. P. Mueller, L. Rudig, Ultrasound-guided spinal fracture repositioning, ligamentotaxis, and remodeling after thoracolumbar burst fractures, Spine 31 (2006) E739–E746.

[7] H.-E. Gueziri, C. Santaguida, D. L. Collins, The state-of-the-art in ultrasound-guided spine interventions, Medical Image Analysis 65 (2020) 101769.

[8] J. L. Herring, B. M. Dawant, C. R. Maurer, D. M. Muratore, R. L. Galloway, J. Michael Fitzpatrick, Surface-based registration of CT images to physical space for image-guided surgery of the spine: A sensitivity study, IEEE Transactions on Medical Imaging 17 (1998) 743–752.

[9] D. M. Muratore, J. H. Russ, B. M. Dawant, R. L. Galloway, Three-dimensional image registration of phantom vertebrae for image-guided surgery: A preliminary study, Computer

Aided Surgery 7 (2002) 342–352.

[10] H. Talib, M. Peterhans, J. Garcia, M. Styner, M. A. Gonzalez Ballester, Information filtering for ultrasound-based real-time registration., IEEE transactions on biomedical engineering 58 (2011) 531–540.

[11] B. Brendel, S. W. A. Rick, M. Stockheim, H. Ermert, Registration of 3d ct and ultrasound datasets of the spine using bone structures, Computer Aided Surgery 7 (2002) 146–155.

[12] S. Gill, P. Abolmaesumi, G. Fichtinger, J. Boisvert, D. Pichora, D. Borshneck, P. Mousavi, Biomechanically constrained groupwise ultrasound to CT registration of the lumbar spine, Medical Image Analysis 16 (2012) 662–674.

[13] A. Rasoulian, P. Abolmaesumi, P. Mousavi, Feature-based multibody rigid registration of CT and ultrasound images of lumbar spine, Medical Physics 39 (2012) 3154–3166.

[14] L. Ma, Z. Zhao, F. Chen, B. Zhang, L. Fu, H. Liao, Augmented reality surgical navigation with ultrasound-assisted registration for pedicle screw placement: a pilot study., International journal of computer assisted radiology and surgery 12 (2017) 2205–2215.

[15] C. X. B. Yan, B. Goulet, S. J.-S. Chen, D. Tampieri, D. L. Collins, Validation of automated ultrasound-CT registration of vertebrae, International Journal of Computer Assisted Radiology and Surgery 7 (2012 a) 601–610.

[16] C. X. Yan, B. Goulet, D. Tampieri, D. L. Collins, Ultrasound-CT registration of vertebrae without reconstruction, International Journal of Computer Assisted Radiology and Surgery 7 (2012 b) 901–909.

[17] T. K. Koo, W. E. Kwok, Hierarchical CT to Ultrasound Registration of the Lumbar Spine: A Comparison with Other Registration Methods, Annals of Biomedical Engineering 44 (2016) 2887–2900.

[18] H.-E. Gueziri, S. Drouin, C. X. B. Yan, D. L. Collins, Toward real-time rigid registration of intra-operative ultrasound with preoperative ct images for lumbar spinal fusion surgery, International Journal of Computer Assisted Radiology and Surgery 14 (2019) 1933–1943.

[19] H.-E. Gueziri, O. Rabau, C. Santaguida, D. L. Collins, Evaluation of an ultrasound-based navigation system for spine neurosurgery: a porcine cadaver study, Front. Oncol. 11:619204 (2021).

[20] S. Nagpal, P. Abolmaesumi, A. Rasoulian, I. Hacihaliloglu, T. Ungi, J. Osborn, V. A. Lessoway, J. Rudan, M. Jaeger, R. N. Rohling, D. P. Borschneck, P. Mousavi, A multi-vertebrae ct to us registration of the lumbar spine in clinical data, International Journal of Computer Assisted Radiology and Surgery 10 (2015) 1371–1381.

[21] D. Behnami, A. Seitel, A. Rasoulian, E. M. A. Anas, V. Lessoway, J. Osborn, R. Rohling, P. Abolmaesumi, Joint registration of ultrasound, CT and a shape+pose statistical model of the lumbar spine for guiding anesthesia., International journal of computer assisted radiology and surgery 11 (2016) 937–945.

[22] D. Behnami, A. Sedghi, E. M. A. Anas, A. Rasoulian, A. Seitel, V. Lessoway, T. Ungi, D. Yen, J. Osborn, P. Mousavi, R. Rohling, P. Abolmaesumi, Model-based registration of preprocedure MR and intraprocedure US of the lumbar spine, International Journal of Computer Assisted Radiology and Surgery 12 (2017) 973–982.

[23] F. Chen, D. Wu, H. Liao, Registration of CT and ultrasound images of the Spine with neural network and orientation code mutual information, Lecture Notes in Computer Science (including subseries Lecture Notes in Artificial Intelligence and Lecture Notes in Bioinformatics) 9805 LNCS (2016) 292–301.

[24] S. Winter, B. Brendel, I. Pechlivanis, K. Schmieder, C. Igel, Registration of ct and intraoperative 3-d ultrasound images of the spine using evolutionary and gradient-based methods, IEEE Transactions on Evolutionary Computation 12 (2008) 284–296.

[25] H.-E. Gueziri, C. X. Yan, D. L. Collins, Open-source software for ultrasound-based guidance in spinal fusion surgery. Ultrasound Med Biol 2020;46:3353–68.

[26] S. Drouin, A. Kochanowska, M. Kersten-Oertel, I. J. Gerard, R. Zelmann, D. De Nigris, S. Bériault, T. Arbel, D. Sirhan, A. F. Sadikot, J. A. Hall, D. S. Sinclair, K. Petrecca, R. F. DelMaestro, D. L. Collins, IBIS: an OR ready open-source platform for image-guided neurosurgery, International Journal of Computer Assisted Radiology and Surgery 12 (2017) 363–378.

[27] A. Lasso, T. Heffter, A. Rankin, C. Pinter, T. Ungi, G. Fichtinger, Plus: Open-source toolkit for ultrasound-guided intervention systems, IEEE Transactions on Biomedical Engineering (2014) 2527–2537. doi: 10.1109/TBME.2014.2322864.

[28] L. Mercier, R. F. Del Maestro, K. Petrecca, A. Kochanowska, S. Drouin, C. X. Yan, A. L.

Janke, S. J.-S. Chen, D. L. Collins, New prototype neuronavigation system based on preoperative imaging and intraoperative freehand ultrasound: system description and validation, International journal of computer assisted radiology and surgery 6 (2011) 507–522.

[29] A. Fedorov, R. Beichel, J. Kalpathy-Cramer, J. Finet, J.-C. Fillion-Robin, S. Pujol, C. Bauer, D. Jennings, F. Fennessy, M. Sonka, et al., 3d slicer as an image computing platform for the quantitative imaging network, Magnetic resonance imaging 30 (2012) 1323–1341.

[30] C. X. Yan, B. Goulet, J. Pelletier, S. J. S. Chen, D. Tampieri, D. L. Collins, Towards accurate, robust and practical ultrasound-CT registration of vertebrae for image-guided spine surgery, International Journal of Computer Assisted Radiology and Surgery 6 (2011) 523–537.

[31] W. Schroeder, K. Martin, B. Lorensen, The Visualization Toolkit (4th ed.), Kitware, 2006.

[32] A. Aoude, M. Fortin, R. Figueiredo, P. Jarzem, J. Ouellet, M. H. Weber, Methods to determine pedicle screw placement accuracy in spine surgery: a systematic review, European Spine Journal 24 (2015) 990–1004.

[33] P. J. Belmont Jr, W. R. Klemme, A. Dhawan, D. W. Polly Jr, In vivo accuracy of thoracic pedicle screws, Spine 26 (2001) 2340–2346.

[34] D. Guha, R. Jakubovic, S. Gupta, N. M. Alotaibi, D. Cadotte, L. B. da Costa, R. George, C. Heyn, P. Howard, A. Kapadia, J. M. Klostranec, N. Phan, G. Tan, T. G. Mainprize, A. Yee, V. X. Yang, Spinal intraoperative three-dimensional navigation: correlation between clinical and absolute engineering accuracy, Spine Journal 17 (2017) 489–498.

[35] A. Aoude, S. Ghadakzadeh, H. Alhamzah, M. Fortin, P. Jarzem, J. A. Ouellet, M. H. Weber, Postoperative assessment of pedicle screws and management of breaches: A survey among canadian spine surgeons and a new scoring system, Asian Spine J 12 (2018) 37–46.

[36] Y. Sakai, Y. Matsuyama, H. Nakamura, Y. Katayama, S. Imagama, Z. Ito, N. Ishiguro, Segmental pedicle screwing for idiopathic scoliosis using computer-assisted surgery, Clinical Spine Surgery 21 (2008) 181–186.

[37] N.-F. Tian, H.-Z. Xu, Image-guided pedicle screw insertion accuracy: a meta-analysis, International orthopaedics 33 (2009) 895–903.

[38] E. Van de Kelft, F. Costa, D. Van der Planken, F. Schils, A prospective multicenter

registry on the accuracy of pedicle screw placement in the thoracic, lumbar, and sacral levels with the use of the o-arm imaging system and stealthstation navigation, Spine 37 (2012) E1580–E1587.

[39] B. D. Kim, W. K. Hsu, G. S. De Oliveira Jr, S. Saha, J. Y. Kim, Operative duration as an independent risk factor for postoperative complications in single-level lumbar fusion: an analysis of 4588 surgical cases, Spine 39 (2014) 510–520.

[40] S. Rajasekaran, M. Bhushan, S. Aiyer, R. Kanna, A. P. Shetty, Accuracy of pedicle screw insertion by airo intraoperative ct in complex spinal deformity assessed by a new classification based on technical complexity of screw insertion, European Spine Journal 27 (2018) 2339–2347.

[41] K. Cleary, J. Anderson, M. Brazaitis, G. Devey, A. DiGioia, M. Freedman, D. Grönemeyer, C. Lathan, H. Lemke, D. Long, S. Mun, R. Taylor, Final report of the technical requirements for image-guided spine procedures workshop, Computer Assisted Surgery 5 (2000) 180–215.

[42] Y. R. Rampersaud, D. A. Simon, K. T. Foley, Accuracy requirements for image-guided spinal pedicle screw placement, Spine 26 (2001) 352–359.

[43] J. M. Fitzpatrick, J. B. West, The distribution of target registration error in rigid-body point-based registration, IEEE transactions on medical imaging 20 (2001) 917–927.

[44] R. Dath, A. Ebinesan, K. Porter, A. Miles, Anatomical measurements of porcine lumbar vertebrae, Clinical biomechanics (Bristol, Avon) 22 (2007) 607–613.

[45] S.-R. Sheng, X.-Y. Wang, H.-Z. Xu, G.-Q. Zhu, Y.-F. Zhou, Anatomy of large animal spines and its comparison to the human spine: a systematic review, European Spine Journal 19 (2010) 46–56.

[46] S.-B. Lien, N.-H. Liou, S.-S. Wu, Analysis of anatomic morphometry of the pedicles and the safe zone for through-pedicle procedures in the thoracic and lumbar spine, European Spine Journal 16 (2007) 1215–1222.

[47] A. Lang, P. Mousavi, S. Gill, G. Fichtinger, P. Abolmaesumi, Multi-modal registration of speckle-tracked freehand 3D ultrasound to CT in the lumbar spine, Medical Image Analysis 16 (2012) 675–686.

[48] D. Mendelsohn, J. Strelzow, N. Dea, N.L. Ford, J. Batke, A. Pennington, K. Yang, T. Ailon,

M. Boyd, M. Dvorak, B. Kwon, Patient and surgeon radiation exposure during spinal instrumentation using intraoperative computed tomography-based navigation. The Spine Journal 16 (2016) 343–354.

[49] S. R. Kantelhardt, C. H. Bock, J. Larsen, V. Bockermann, W. Schillinger, V. Rohde, A. Giese, Intraosseous ultrasound in the placement of pedicle screws in the lumbar spine. Spine 34.4 (2009): 400-407.

[50] S.R. Kantelhardt, et al. Intra-osseous ultrasound for pedicle screw positioning in the subaxial cervical spine: an experimental study. Acta neurochirurgica 152.4 (2010): 655-661.

[51] A.H. Aly, H. J. Ginsberg, R. S. C. Cobbold. On ultrasound imaging for guided screw insertion in spinal fusion surgery. Ultrasound in medicine & biology 37.4 (2011): 651-664.